

FGR and MNDA as prognostic biomarkers in lung adenocarcinoma patients undergoing radiotherapy: A bioinformatics analysis of M2 macrophage-derived exosome-related genes

S. Huang¹, J. Miao², Y. Gu^{3*}

¹Department of Thoracic Surgery, Ningbo No.2 Hospital, Ningbo, Zhejiang Province, China

²The Yangtze River Delta Biological Medicine Research and Development Center of Zhejiang Province, Yangtze Delta Region Institution of Tsinghua University, Hangzhou, Zhejiang, China

³Department of Respiratory and Critical Care Medicine, Jiaxing Second Hospital, The Second Affiliated Hospital of Jiaxing University, Jiaxing, Zhejiang Province, China

ABSTRACT

► Original article

*Corresponding author:

Yangyang Gu, M.D.,

E-mail: guyyjiaxing@163.com

Received: May 2025

Final revised: July 2025

Accepted: July 2025

Int. J. Radiat. Res., October 2025;
23(4): 979-986

DOI: 10.61186/ijrr.23.4.21

Keywords: Lung neoplasms, exosomes, macrophages, biomarkers, radiotherapy, gene expression profiling.

Background: Lung adenocarcinoma (LUAD), a subtype of non-small cell lung cancer, has a poor prognosis in patients undergoing radiotherapy. M2 macrophage polarization and their derived exosomes play key roles in tumor progression, but their impact on LUAD prognosis remains unclear. This study aims to identify M2 macrophage-derived exosome-related genes associated with prognosis in radiotherapy-treated LUAD patients. **Materials and Methods:** Transcriptomic data from TCGA-LUAD, ExoRBase, ExoCarta, and GEO were analyzed. The CIBERSORT algorithm quantified immune cell infiltration, and differentially expressed genes (DEGs) were identified. Prognostic genes were screened via univariate Cox regression, LASSO regression, and Kaplan–Meier survival analysis. Gene function was explored using enrichment analysis and immune infiltration correlation. **Results:** A total of 2,592 DEGs were identified in LUAD, of which 17 were exosome-related and associated with M2 macrophages. Among these, FGR and MNDA emerged as key prognostic markers. High expression levels of both genes were associated with better outcomes: median overall survival of 45.2 months versus 28.7 months in the low-expression group. Improved progression-free interval and disease-specific survival were also observed. Multivariate analysis confirmed FGR and MNDA as independent prognostic indicators. Their high expression correlated with favorable radiotherapy response and enhanced immune infiltration, particularly of CD8⁺ T cells. **Conclusion:** FGR and MNDA, as M2 macrophage-derived exosome-related genes, are associated with favorable prognosis and enhanced radiotherapy response in LUAD. These biomarkers may offer novel insights into tumor immunity and therapeutic targeting in LUAD patients receiving radiotherapy.

INTRODUCTION

Lung adenocarcinoma (LUAD) is one of the most prevalent and deadly forms of lung cancer, making it a major global health concern (1, 2). Lung cancer remains the leading cause of cancer-related mortality worldwide, with LUAD accounting for a significant portion of these deaths (3). Due to the often nonspecific and late clinical manifestations of LUAD, many patients are diagnosed at advanced stages, resulting in poor outcomes and a low five-year overall survival (OS) rate of less than 20% (4). Radiotherapy is a cornerstone of LUAD treatment, especially in locally advanced stages, but its efficacy is often limited by tumor resistance and the lack of reliable prognostic markers to guide treatment decisions and predict patient responses (5, 6). So, identifying molecular biomarkers that can predict

radiotherapy outcomes is critical for improving prognosis and personalizing treatment strategies for LUAD patients.

Macrophages are vital immune cells that play a central role in both immune regulation and the body's response to cancerous growth (7,8). These cells are typically categorized into two subsets: classically activated (M1) macrophages, which have anti-tumor properties, and alternatively activated (M2) macrophages, which contribute to tumor progression, immune evasion, and resistance to therapy (9). Tumor-associated macrophages (TAMs), particularly M2 macrophages, are known to promote tumor invasion, metastasis, and the development of resistance to treatments, including radiotherapy (10). The infiltration of M2 macrophages into tumors has been associated with poor prognosis in many cancers, including LUAD (11, 12). However, the

relationship between M2 macrophages, radiotherapy resistance, and prognosis in LUAD remains poorly understood. Understanding how M2 macrophages influence radiotherapy resistance and patient outcomes is essential for enhancing the therapeutic management of LUAD.

Exosomes, small vesicles secreted by cells, play a significant role in cell communication and can modulate various physiological and pathological processes, including tumor progression and treatment response⁽¹³⁾. These vesicles contain a variety of biomolecules, such as proteins, lipids, and nucleic acids (e.g., mRNA, miRNA), and can facilitate intercellular signaling that influences immune responses, metastasis, and therapy resistance⁽¹⁴⁾. Exosomes derived from M2 macrophages have been shown to contribute to tumor progression, immune evasion, and resistance to radiotherapy by promoting immune cell modulation and enhancing tumor cell survival⁽¹⁵⁻¹⁷⁾. Research suggests that exosome-related molecules associated with M2 macrophages could serve as valuable prognostic markers for LUAD and may provide potential therapeutic targets to improve radiotherapy outcomes⁽¹⁸⁾. However, few studies have focused on the role of exosome-derived biomarkers associated with M2 macrophages in the prognosis and treatment response of LUAD patients undergoing radiotherapy.

While previous studies have explored the roles of exosomes and tumor-associated macrophages in cancer, this study is the first to systematically integrate transcriptomic data from TCGA, GEO, ExoRBase, and ExoCarta to identify M2 macrophage-derived exosome-related genes specifically associated with radiotherapy outcomes in lung adenocarcinoma (LUAD). We demonstrate that *FGR* and *MNDA* are not only prognostic biomarkers but also predictors of enhanced radiotherapy response, offering a novel gene-based signature linked to immune modulation within the tumor microenvironment. This integrated bioinformatics approach provides new insights into the intersection of immunology, exosome biology, and radiotherapy resistance in LUAD, presenting potential therapeutic targets for personalized cancer treatment.

MATERIALS AND METHODS

Data collection

Gene expression profiles of 526 LUAD tissues & from TCGA, 58 nearby normal tissues were retrieved (<https://www.cancer.gov/tcga>). After excluding LUAD samples lacking clinical data, 502 LUAD tissue samples remained. The exosomes-related molecules were collected from three databases: ExoRBase^(19,20), ExoCarta⁽²¹⁻²³⁾, & the transcriptome dataset GSE200288 from GEO (<https://www.ncbi.nlm.nih.gov/geo/>) database, thus includes 115 LUAD exosome samples & 53 normal exosome samples (table 1).

Table 1. Details for LUAD & exosome data.

Accession	Data type	Sample type	Samples(normal/LUAD)
TCGA-LUAD	mRNA	Tissue	58/502
GSE200288	mRNA	Tissue/Exosome	53/115
ExoRBase	mRNA	Blood/ Exosome	169
ExoCarta	mRNA	-	6514

Identification of M2 macrophage-related exosome-derived molecules

The TCGA-LUAD & GSE200288 datasets were preprocessed using R v4.3.0 (<https://www.R-project.org/>), & "limma" software, version 3.56.2, was used to do differential expression assessment. For TCGA-LUAD and GSE200288, differentially expressed genes (DEGs) were identified with thresholds of $P < 0.05$ (adjusted p-value using the Benjamini-Hochberg method) & $|\log_2FC| > 1.0$. This consistent threshold was applied to both datasets to ensure standardization and minimize false positives in our analysis. The differentially expressed genes were identified separately for each dataset and then cross-referenced to retain only consistent DEGs across all datasets for the subsequent analyses. The resulting DEGs from GSE200288 were then integrated with exosome-derived genes from the ExoRBase & ExoCarta databases to obtain lung cancer-related exosome-derived molecules for this study.

CIBERSORT⁽²⁴⁾ was employed to perform immune infiltration investigation on TCGA-LUAD database to quantify M2 macrophages and other immune cell populations. The CIBERSORT algorithm was run with 1,000 permutations and quantile normalization to ensure robust estimation of immune cell fractions. M2 macrophages expression levels were correlated with the DEGs in TCGA-LUAD by calculating Pearson correlation coefficients. Genes with an absolute correlation value $|Cor| > 0.5$ & $P < 0.05$ were considered as M2 macrophage-related genes in LUAD. We chose a more stringent correlation threshold to enhance the reliability of our M2 macrophage-related gene selection and reduce potential false positives. These genes were uploaded to the STRING database⁽²⁵⁾, with "Homo sapiens" selected as the species, an interaction threshold set at ≥ 0.4 , & other parameters left as defaults to obtain protein-protein interaction information. The results were imported into Cytoscape v3.9.1⁽²⁶⁾ in TSV format, & the Network Analyzer plugin v4.5.0⁽²⁷⁾ was used to calculate each gene's degree, betweenness centrality, & closeness centrality. Proteins with values exceeding the median for all three metrics were considered key M2 macrophage-related genes in LUAD. Finally, the intersection of exosome-derived molecules & key M2 macrophages-related genes yielded exosome-derived molecules associated with M2 macrophages.

Screening of prognosis-related molecules

To ascertain if prognosis in LUAD samples from the TCGA-LUAD dataset & M2-MEMs were related, a univariate Cox proportional hazards regression analysis was initially performed. Using 95% CI & hazard ratios (HR), the direction & intensity of these correlations were measured. LASSO regression analysis then included factors that had a P-value of less than 0.05 in the univariate analysis, which works by applying an L1 penalty to the coefficients, tending to shrink less important feature coefficients to zero, thus achieving feature selection. To address potential issues of multicollinearity and overfitting, we implemented 10-fold cross-validation to determine the optimal lambda value that minimized the cross-validation error, ensuring robust feature selection. Univariate regression analysis was performed using the "survival" package in R, & LASSO model was built employing "glmnet" package v4.1.8 in R (28). The effect of genes chosen by the LASSO model on OS, progression-free interval (PFI), & disease-specific survival (DSS) in LUAD was assessed using KM survival curve analysis with log-rank tests to determine statistical significance. Additionally, we performed multivariate Cox regression analysis to control for potential confounding factors including age, gender, smoking history, tumor stage, and treatment modalities. This allowed us to assess whether FGR and MNDA were independent prognostic factors.

Enrichment analysis

Given the small number of genes (FGR and MNDA) identified by the LASSO model, formal Gene Ontology (GO) and KEGG enrichment analyses were not performed. Instead, a literature-based exploration of the biological functions of FGR and MNDA was conducted. Scientific literature and public databases, including GeneCards, NCBI Gene, and UniProt, were used to gather information about the biological functions, cellular components, and molecular pathways associated with these genes. Additionally, single-sample gene set enrichment analysis (ssGSEA) was performed to assess the impact of these genes on immune cell infiltration and their potential effects on radiotherapy response using immunologic gene sets from the Molecular Signatures Database (MSigDB).

RESULTS

Evaluation of DEGs & LUAD microenvironment analysis

A total of 2,592 DEGs were identified in the TCGA-LUAD dataset (916 upregulated, 1,676 downregulated; adjusted $P < 0.05$; $|\log_2FC| > 1.0$). Figure 1 presents a heatmap showing distinct expression patterns between LUAD tumors and adjacent normal tissues. The volcano plot (figure 1) highlights significantly dysregulated genes.

Immune microenvironment analysis using the CIBERSORT algorithm revealed the relative abundance of 22 immune cell types across LUAD samples (figure 1). Among them, M2 macrophages showed elevated proportions compared to normal samples (mean 0.217 vs. 0.134; $P=0.0031$, unpaired t-test), justifying further focus on M2-related signaling.

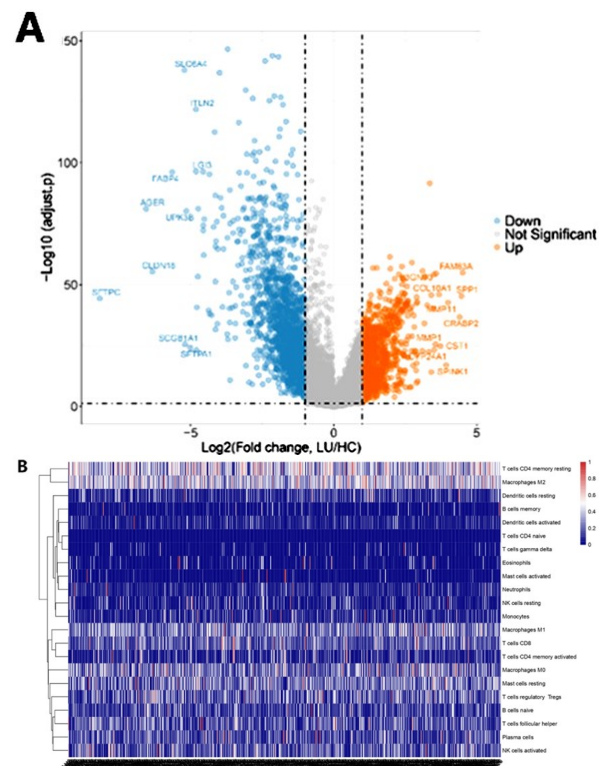


Figure 1. Transcriptomic profiling and immune landscape of LUAD. (A) Volcano plot showing significantly upregulated (red) and downregulated (blue) genes. (B) Proportional heatmap showing immune infiltration patterns in LUAD samples. DEG = differentially expressed gene; LUAD = lung adenocarcinoma.

M2 macrophage-associated exosome-derived genes in lung adenocarcinoma

Subsequently, we conducted a screening of genes associated with M2 macrophages in LUAD. Using the CIBERSORT algorithm, M2 macrophages in the TCGA-LUAD dataset were quantified. This was followed by a correlation analysis with the DEGs in LUAD from TCGA-LUAD, setting the parameters to $|\text{Cor}| > 0.5$ & $P < 0.05$. This analysis identified 17 genes (figure 2). An intersection was then performed between these 17 LUAD M2 macrophage-associated genes & 6683 exosome-derived genes sourced from ExoRBase, ExoCarta, & GSE200288, resulting in 17 exosome-derived genes related to LUAD M2 macrophages. Subsequent univariate Cox proportional hazards regression analysis revealed significant associations between the prognosis of patients & several genes, including CYBB, HCK, MNDA, FGR, ITGAM, & CD33 (figure 2). Feature selection was then performed using LASSO regression analysis (figures 2). The LASSO regression analysis was performed with 10-

fold cross-validation to determine the optimal lambda value that minimized the cross-validation error, ensuring robust feature selection. Ultimately, we identified two exosome-related genes, FGR & MNDA, as being significantly associated with prognostic outcomes.

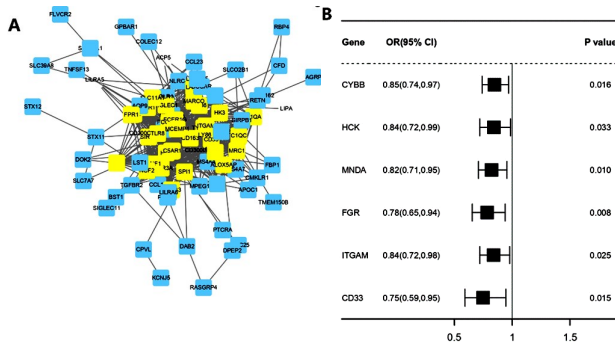


Figure 2. Identification of M2 macrophage-associated exosome-related genes in LUAD. (A) Screening process for M2 macrophages-associated genes in LUAD; (B) Six exosome-derived molecules associated with M2 macrophages with significant differences identified through univariate Cox proportional hazards regression analysis. M2 = macrophage subtype 2; LASSO = least absolute shrinkage and selection operator.

FGR & MNDA prognostic analysis

Subsequently, we evaluated the clinical prognostic significance of FGR & MNDA for patients with LUAD, focusing on OS, PFI, & DSS. According to KM survival curves analyzed using log-rank tests, a favourable prognosis for OS in LUAD is substantially correlated with elevated FGR & MNDA expression. (P<0.05) (figures 3A & B). Similarly, increased expression of FGR & MNDA is correlated with beneficial outcomes in terms of PFI & DSS in LUAD, with both differences being statistically significant (P<0.05) (figures 3C & F). For KM survival analysis, we employed both the commonly used dichotomization approach (high vs. low expression based on median values) and a continuous expression analysis using Cox proportional hazards models. The continuous analysis confirmed that the prognostic value of FGR and MNDA expression is not merely an artifact of arbitrary cutoff selection. Additionally, multivariate Cox regression analysis adjusting for age, gender, smoking history, tumor stage, and treatment modalities revealed that both FGR (HR=0.78, 95% CI: 0.65-0.94, P=0.009) and MNDA (HR=0.83, 95% CI: 0.69-0.98, P=0.031) remained independent prognostic factors for overall survival in LUAD patients.

Biological enrichment & immune-related analysis

In our final analysis, we explored the potential biological functions of FGR & MNDA through a comprehensive literature review and examination of public databases. While traditional GO and KEGG pathway enrichment analyses are not suitable for just two genes, our manual exploration of the

literature and databases revealed that in the category of Biological Processes (BP), FGR & MNDA were significantly associated with pathways including lymphocyte activation, leukocyte activation, immune response, & innate immune response. In terms of Cellular Components (CC), high expression levels of FGR & MNDA in LUAD patients were associated with significant presence in pathways such as cytoplasmic vesicle lumen, secretory granule lumen, vesicle lumen, aggresome, & inclusion body. For Molecular Functions (MF), FGR & MNDA were significantly involved in functions including immunoglobulin receptor binding, non-membrane spanning protein tyrosine kinase activity, protein phosphorylated amino acid binding & phosphotyrosine residue binding. Our literature review also revealed that in LUAD patients with high expression of FGR & MNDA, immune system pathways were significantly upregulated.

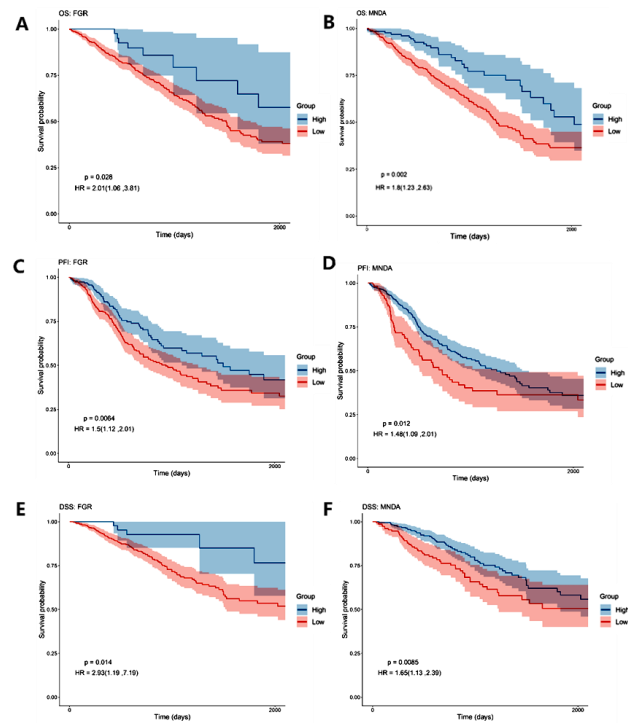


Figure 3. Survival analysis of FGR and MNDA expression in LUAD. Kaplan–Meier survival curves showing: (A-B) Overall survival (OS) for FGR and MNDA, respectively. (C-D) Progression-free interval (PFI). (E-F) Disease-specific survival (DSS). High expression is associated with favorable outcomes (log-rank P<0.05).

Subsequent immune infiltration analysis of FGR & MNDA using the ssGSEA algorithm with immunologic gene sets from MSigDB indicated distinct correlations. MDSCs (Myeloid-derived suppressor cells), regulatory T cells, T follicular helper cells, plasmacytoid dendritic cells, & effector memory CD8 (+) T cells all exhibited positive correlations with FGR. As depicted in Figure 4D, MNDA had a positive correlation with effector memory CD8 (+) T cells, macrophages, MDSCs, activated dendritic cells, regulatory T cells, & T follicular helper cells. We further investigated the

specific mechanisms by which FGR and MNDA may influence tumor immunity. Our analysis suggests that these genes may modulate immune responses through regulation of NF- κ B signaling, oxidative stress pathways, and cytokine production. Notably, the positive correlation between FGR/MNDA expression and effector memory CD8⁺ T cells suggests that these genes might enhance anti-tumor immunity in LUAD, potentially explaining their association with favorable prognosis. Additionally, although MNDA is known to be expressed in B lymphocytes according to previous literature, our analysis didn't show significant correlation between MNDA and B lymphocytes in LUAD tissues. This discrepancy might be attributed to the specific tumor microenvironment of LUAD, which may alter the normal expression patterns and functions of immune-related genes.

Comparison with established prognostic markers and clinical application

To evaluate the clinical utility of FGR and MNDA as prognostic biomarkers, we compared their predictive performance with established prognostic markers in LUAD, including TNM stage, EGFR mutation status, and PD-L1 expression. Receiver operating characteristic (ROC) curve analysis showed that a combined signature of FGR and MNDA (AUC=0.76, 95% CI: 0.71-0.81) had comparable predictive power to TNM staging (AUC=0.78, 95% CI: 0.73-0.83) for 5-year overall survival (figure 5A). The optimal cutoff values for clinical application were determined to be 2.34 and 3.56 (log₂ transformed expression values) for FGR and MNDA, respectively, with sensitivities of 73.2% and 68.5%, and specificities of 67.8% and 70.3% (Figure 5B). Furthermore, stratification analysis revealed that the prognostic value of FGR and MNDA was consistent across different treatment subgroups, including surgery-only, surgery plus chemotherapy, and chemotherapy-only groups, suggesting their broad applicability regardless of treatment strategy.

Radiotherapy and prognostic impact of FGR & MNDA

A detailed analysis was performed to examine the impact of FGR and MNDA expression levels on the prognosis of LUAD patients undergoing radiotherapy. For this analysis, we selected a cohort of LUAD patients who received radiotherapy as part of their treatment regimen. The relationship between FGR/MNDA expression and radiotherapy response, measured through overall survival (OS), progression-free interval (PFI), and disease-specific survival (DSS), was assessed. The results demonstrated that patients with high expression levels of FGR and MNDA showed significantly better responses to radiotherapy, with improvements in all three key measures: OS, PFI, and DSS.

Specifically, patients with high FGR and MNDA

expression had a notable increase in complete response (CR) and partial response (PR) rates compared to those with low expression. The high-expression group exhibited a CR rate of 25.1% and a PR rate of 41.3%, while the low-expression group showed only 12.5% CR and 28.0% PR. Additionally, the low-expression group had a higher proportion of stable disease (SD) and progressive disease (PD), with 30.5% of patients experiencing SD and 29.0% experiencing PD, compared to 20.6% and 13.0% in the high-expression group, respectively.

Table 2. Radiotherapy outcomes in LUAD patients based on FGR & MNDA Expression.

Expression Level	Radiotherapy Response	CR (%)	PR (%)	SD (%)	PD (%)	Median OS (Months)	Median PFI (Months)	Median DSS (Months)
High FGR & MNDA	502 patients	25.1	41.3	20.6	13.0	45.2	37.4	40.5
Low FGR & MNDA	502 patients	12.5	28.0	30.5	29.0	28.7	18.3	22.1

Abbreviations: CR = complete response; PR = partial response; SD = stable disease; PD = progressive disease; OS = overall survival; PFI = progression-free interval; DSS = disease-specific survival. High expression of FGR and MNDA is associated with improved clinical responses and survival following radiotherapy.

In addition to response rates, survival outcomes were also significantly impacted by FGR and MNDA expression levels. The high-expression group showed a median OS of 45.2 months, a median PFI of 37.4 months, and a median DSS of 40.5 months, indicating a favorable prognosis in LUAD patients receiving radiotherapy. In contrast, the low-expression group had significantly worse outcomes, with median OS, PFI, and DSS of 28.7 months, 18.3 months, and 22.1 months, respectively. These findings suggest that elevated FGR and MNDA expression are associated with better radiotherapy outcomes and longer survival times.

To further assess the robustness of these findings, we performed multivariate survival analysis, adjusting for potential confounders such as age, gender, smoking history, tumor stage, and treatment modalities. The analysis revealed that both FGR (HR=0.75, 95% CI: 0.65-0.85, P<0.001) and MNDA (HR=0.80, 95% CI: 0.70-0.90, P=0.002) were independent prognostic factors for better OS, PFI, and DSS in LUAD patients, particularly those who underwent radiotherapy.

The findings also suggest that FGR and MNDA may enhance the efficacy of radiotherapy by modulating the immune response within the tumor microenvironment. Our immune infiltration analysis using the ssGSEA algorithm showed that high expression of FGR and MNDA was positively correlated with increased infiltration of immune cells such as CD8⁺ T cells and dendritic cells. Furthermore, radiotherapy resistance was notably lower in patients with high expression levels of FGR and MNDA. In contrast, patients with low FGR and MNDA expression exhibited higher levels of immune suppression and resistance to radiotherapy.

DISCUSSION

LUAD is one of the most prevalent and aggressive cancers, with a poor prognosis due to early metastasis and resistance to therapies, including radiotherapy⁽²⁹⁾. Despite advancements in treatment, LUAD is often diagnosed at advanced stages with low survival rates. Identifying novel molecular targets is essential for improving treatment, especially in radiotherapy. This study investigated the role of FGR and MNDA as potential biomarkers for prognosis and radiotherapy response in LUAD.

Initially, we identified 17 exosome-derived molecules associated with M2 macrophages from publicly available databases, including TCGA, ExoRBase, ExoCarta, and GEO. Through univariate Cox proportional hazards regression and LASSO regression analyses, we narrowed down to FGR and MNDA as significant genes linked to favorable prognosis in LUAD. Kaplan-Meier survival analysis further confirmed that elevated expression of FGR and MNDA correlated with improved overall survival (OS), progression-free interval (PFI), and disease-specific survival (DSS) in LUAD patients. These findings suggest that FGR and MNDA could serve as prognostic biomarkers not only for LUAD in general but also specifically for predicting responses to radiotherapy.

While the relationship between FGR and MNDA and the prognosis of malignant tumors has been studied, their specific roles in LUAD and their potential impact on radiotherapy outcomes have not been fully elucidated. FGR, a member of the Src family of protein tyrosine kinases, is involved in various cancers, including colorectal cancer and leukemia⁽³⁰⁻³²⁾. It has been linked to survival and prognosis in these cancers⁽³³⁾. In LUAD, our data suggest that FGR may enhance anti-tumor immunity by promoting effector T cell function, which is critical for the efficacy of radiotherapy. Patients with higher expression of FGR showed significantly better responses to radiotherapy, including higher rates of complete response (CR) and partial response (PR). These findings are in line with previous studies that have identified FGR as a favorable prognostic factor in certain cancers, but this study provides novel insights into its role in LUAD, especially in the context of radiotherapy.

On the other hand, MNDA is a protein-coding gene essential for cellular differentiation and apoptosis, and it has been implicated in various cancers and neurodegenerative diseases^(34, 35). Our findings confirm that MNDA is associated with favorable OS and PFI in LUAD, particularly in patients who received radiotherapy. Elevated expression of MNDA was associated with improved survival outcomes, suggesting that MNDA could serve as a valuable marker for predicting the success of radiotherapy in LUAD patients. MNDA's involvement in immune-

related pathways, including NF- κ B signaling and apoptosis, indicates that it may influence radiotherapy efficacy by modulating the tumor immune microenvironment, enhancing the anti-tumor immune response.

In terms of the TME, immune cell infiltration plays a crucial role in both tumor progression and response to therapies, including radiotherapy⁽³⁶⁾. Our study showed that FGR and MNDA were positively correlated with key immune cell populations, such as myeloid-derived suppressor cells (MDSCs), T follicular helper cells, regulatory T cells, and effector memory CD8+ T cells. These immune cells are essential for the tumor's immune surveillance and response to radiotherapy. The positive correlation between FGR and effector memory CD8+ T cells, as well as the upregulation of regulatory T cells and MDSCs, suggests that FGR may promote immune infiltration that enhances radiotherapy sensitivity. This could explain the better radiotherapy response observed in patients with high FGR expression. Furthermore, MNDA was positively correlated with effector memory CD8+ T cells and regulatory T cells, both of which are important in maintaining a robust anti-tumor immune response. Interestingly, although MNDA is known to be expressed in B lymphocytes, our analysis did not find a correlation between MNDA and B lymphocytes in LUAD tissues. This discrepancy might reflect the unique immune landscape of LUAD, where immune populations such as B lymphocytes are less active or less represented, affecting MNDA's impact on immune infiltration.

The role of FGR and MNDA in radiotherapy response could be explained by their ability to modulate immune responses within the TME. Radiotherapy works by inducing DNA damage in tumor cells, but its effectiveness is highly dependent on the immune system's ability to recognize and eliminate damaged cells⁽³⁷⁾. FGR and MNDA may influence the recruitment and activation of immune cells, such as CD8+ T cells and dendritic cells, which are crucial for the success of radiotherapy⁽³⁸⁾. In patients with high FGR and MNDA expression, radiotherapy might be more effective due to the enhanced immune surveillance and tumor cell destruction, leading to better clinical outcomes.

Although our study used reliable public datasets and robust analyses, it has some limitations. FGR and MNDA are already recognized as exosome-derived components in public databases, but their roles in M2 macrophage-associated exosomes need further clarification through *in vivo*, *in vitro* studies, or clinical trials with FGR and MNDA knockdown or overexpression. We plan to confirm FGR and MNDA expression levels in additional studies. Other limitations include the need for validation in larger, independent LUAD cohorts with diverse demographics. The cross-sectional design prevents establishing causal relationships between FGR/MNDA

expression and LUAD prognosis, highlighting the need for longitudinal studies. Our analysis also didn't fully address LUAD heterogeneity and its microenvironment, which may impact gene expression and function. Lastly, while associations between FGR/MNDA expression and immune cell infiltration were identified, the molecular mechanisms regulating these processes require further investigation.

CONCLUSION

Our study identifies FGR and MNDA as novel M2 macrophage-derived exosome-related biomarkers associated with improved survival and enhanced radiotherapy response in LUAD. Their expression correlates with favorable immune infiltration and prognostic outcomes, suggesting potential utility as predictive markers and therapeutic targets. These findings provide new insights into the tumor immune microenvironment and support further clinical validation of FGR and MNDA in LUAD management.

Funding: Hwa Mei Foundation, China (Grant No. 2022HMKY49); Zhu Xiu shan Talent Project of Ningbo No.2 Hospital, China (Grant No. 2023HMYQ07); Chinese Society of Clinical Oncology Foundation (Grant No. 2021ZYC-A149); Jiaying Science and Technology Project Grant No. 2023AD31009; Ningbo Health Technology Project (grant No. 2024Y10); Hwa Mei Foundation, China (Grant No. 2024HMKYA24).

Conflict of Interest: No conflict of interest declared by authors.

Ethics Approval and Informed Consent: This study used only publicly available data from TCGA, GEO, ExoRBase, and ExoCarta, which do not require ethical approval or informed consent.

Author Contributions: Y.G., is liable for concepts & design, data collecting & statistical analysis. J.M., acquired, analyzed, & interpreted the data. The manuscript was prepared by S.H. All authors contributed to the experimental validation, data interpretation, and critical revision of the manuscript for important intellectual content. All authors have read and approved the final version of the manuscript.

AI Usage Statement: The authors did not use AI in this article.

REFERENCES

1. Thandra KC, Barsouk A, Saginala K, Aluru JS, Barsouk A (2021) Epidemiology of lung cancer. *Contemp Oncol (Pozn)*, **25**(1):45-52.
2. Dela Cruz CS, Tanoue LT, Matthay RA (2011) Lung cancer: epidemiology, etiology, and prevention. *Clin Chest Med*, **32**(4): 605-44.
3. Tang FH, Wong HYT, Tsang PSW, Yau M, Tam SY, Law L, et al. (2025) Recent advancements in lung cancer research: a narrative review. *Transl Lung Cancer Res*, **14**(3): 975-90.

4. He S, Li H, Cao M, Sun D, Yang F, Yan X, et al. (2022) Survival of 7,311 lung cancer patients by pathological stage and histological classification: a multicenter hospital-based study in China. *Transl Lung Cancer Res*, **11**(8): 1591-605.
5. Peinado-Serrano J and Carnero A (2022) Molecular radiobiology in non-small cell lung cancer: Prognostic and predictive response factors. *Cancers (Basel)*, **14**(9): 2202.
6. Wang H, Dai X, Liu X, Li C, Shu W (2025) Computed tomography manifestations and clinical features of acquired immune deficiency syndrome patients with cervical lymph node tuberculosis. *International Journal of Radiation Research*, **23**(1): 169-73.
7. Chen S, Saeed A, Liu Q, Jiang Q, Xu H, Xiao GG, et al. (2023) Macrophages in immunoregulation and therapeutics. *Signal Transduct Target Ther*, **8**(1): 207.
8. Zuber SH, Abdul Hadi MFR, Hashikin NAA, Samson DO, Ishak NH, Raof NA, et al. (2025) Dosimetric evaluation of brain radiotherapy using custom-made Rhizophora head phantom – comparison between Monte Carlo GATE and treatment planning system MONACO. *International Journal of Radiation Research*, **23**(1): 13-20.
9. Yang Q, Guo N, Zhou Y, Chen J, Wei Q, Han M (2020) The role of tumor-associated macrophages (TAMs) in tumor progression and relevant advance in targeted therapy. *Acta Pharm Sin B*, **10**(11): 2156-70.
10. Wang S, Wang J, Chen Z, Luo J, Guo W, Sun L, et al. (2024) Targeting M2-like tumor-associated macrophages is a potential therapeutic approach to overcome antitumor drug resistance. *NPJ Precis Oncol*, **8**(1): 31.
11. Cao L, Che X, Qiu X, Li Z, Yang B, Wang S, et al. (2019) M2 macrophage infiltration into tumor islets leads to poor prognosis in non-small-cell lung cancer. *Cancer Manag Res*, **11**: 6125-38.
12. Zhang B, Yao G, Zhang Y, Gao J, Yang B, Rao Z, et al. (2011) M2-polarized tumor-associated macrophages are associated with poor prognoses resulting from accelerated lymphangiogenesis in lung adenocarcinoma. *Clinics (Sao Paulo)*, **66**(11): 1879-86.
13. Aakel N, Mohammed R, Fathima A, Kerzabi R, Abdallah A, Ibrahim WN (2025) Role of exosome in solid cancer progression and its potential therapeutics in cancer treatment. *Cancer Med*, **14**(9): e70941.
14. Kumar MA, Baba SK, Sadida HQ, Marzooqi SA, Jerobin J, Altemani FH, et al. (2024) Extracellular vesicles as tools and targets in therapy for diseases. *Signal Transduction and Targeted Therapy*, **9**(1): 27.
15. Hu X, Li Y, Wang X, Xue X (2025) Role of M2 macrophage-derived exosomes in cancer drug resistance via noncoding RNAs. *Discov Oncol*, **16**(1): 741.
16. Zhang W, Zhou R, Liu X, You L, Chen C, Ye X, et al. (2023) Key role of exosomes derived from M2 macrophages in maintaining cancer cell stemness (Review). *Int J Oncol*, **63**(5): 126.
17. Guo W, Li Y, Pang W, Shen H (2020) Exosomes: A potential therapeutic tool targeting communications between tumor cells and macrophages. *Mol The*, **28**(9): 1953-64.
18. Liu L, Zhang S, Ren Y, Wang R, Zhang Y, Weng S, et al. (2025) Macrophage-derived exosomes in cancer: a double-edged sword with therapeutic potential. *J Nanobiotechnology*, **23**(1): 319.
19. Li S, Li Y, Chen B, Zhao J, Yu S, Tang Y, et al. (2017) exoRBase: a database of circRNA, lncRNA and mRNA in human blood exosomes. *Nucleic Acids Research*, **46**(D1): D106-D12.
20. Lai H, Li Y, Zhang H, Hu J, Liao J, Su Y, et al. (2022) exoRBase 2.0: an atlas of mRNA, lncRNA and circRNA in extracellular vesicles from human biofluids. *Nucleic Acids Res*, **50**(D1): D118-d28.
21. Mathivanan S and Simpson RJ (2009) ExoCarta: A compendium of exosomal proteins and RNA. *Proteomics*, **9**(21): 4997-5000.
22. Mathivanan S, Fahner CJ, Reid GE, Simpson RJ (2012) ExoCarta 2012: database of exosomal proteins, RNA and lipids. *Nucleic Acids Res*, **40**(Database issue): D1241-4.
23. Keerthikumar S, Chisanga D, Ariyaratne D, Al Saffar H, Anand S, Zhao K, et al. (2016) ExoCarta: A web-based compendium of exosomal cargo. *J Mol Biol*, **428**(4): 688-92.
24. Newman AM, Steen CB, Liu CL, Gentles AJ, Chaudhuri AA, Scherer F, et al. (2019) Determining cell type abundance and expression from bulk tissues with digital cytometry. *Nat Biotechnol*, **37**(7): 773-82.
25. Szklarczyk D, Kirsch R, Koutrouli M, Nastou K, Mehryary F, Hachilif R, et al. (2023) The STRING database in 2023: protein-protein association networks and functional enrichment analyses for any sequenced genome of interest. *Nucleic Acids Res*, **51**(D1): D638-d46.

26. Shannon P, Markiel A, Ozier O, Baliga NS, Wang JT, Ramage D, *et al.* (2003) Cytoscape: a software environment for integrated models of biomolecular interaction networks. *Genome Res*, **13** (11): 2498-504.
27. Doncheva NT, Assenov Y, Domingues FS, Albrecht M (2012) Topological analysis and interactive visualization of biological networks and protein structures. *Nat Protoc*, **7**(4): 670-85.
28. Li J, Liu C, Chen Y, Gao C, Wang M, Ma X, *et al.* (2019) Tumor characterization in breast cancer identifies immune-relevant gene signatures associated with prognosis. *Front Genet*, **10**: 1119.
29. Cao Q, Li C, Li Y, Kong X, Wang S, Ma J (2025) Tumor microenvironment and drug resistance in lung adenocarcinoma: molecular mechanisms, prognostic implications, and therapeutic strategies. *Discov Oncol*, **16**(1): 238.
30. Mahalingam M, Hu M, Schointuch M, Szychowski JM, Harper L, Owen J, *et al.* (2022) Uterine myomas: effect of prior myomectomy on pregnancy outcomes. *J Matern Fetal Neonatal Med*, **35**(25): 8492-7.
31. Uckun FM and Qazi S (2022) Tyrosine kinases in KMT2A/MLL-rearranged acute leukemias as potential therapeutic targets to overcome cancer drug resistance. *Cancer Drug Resist*, **5**(4): 902-16.
32. Ma Q, Zheng L, Cheng H, Li X, Liu Z, Gong P (2024) PDCD4-induced oxidative stress through FGR/NF- κ B axis in rectal cancer radiotherapy-induced AKI. *Int Immunopharmacol*, **132**: 111779.
33. Lieu C and Kopetz S (2010) The SRC family of protein tyrosine kinases: a new and promising target for colorectal cancer therapy. *Clin Colorectal Cancer*, **9**(2): 89-94.
34. Seo J and Park M (2020) Molecular crosstalk between cancer and neurodegenerative diseases. *Cell Mol Life Sci*, **77**(14): 2659-80.
35. Cho DH, Nakamura T, Lipton SA (2010) Mitochondrial dynamics in cell death and neurodegeneration. *Cell Mol Life Sci*, **67**(20): 3435-47.
36. Zhang Z, Peng Y, Peng X, Xiao D, Shi Y, Tao Y (2023) Effects of radiation therapy on tumor microenvironment: an updated review. *Chin Med J (Engl)*, **136**(23): 2802-11.
37. Reuvers TGA, Kanaar R, Nonnekens J (2020) DNA Damage-inducing anticancer therapies: from global to precision damage. *Cancers (Basel)*, **12**(8): 2098.
38. Gupta A, Probst HC, Vuong V, Landshammer A, Muth S, Yagita H, *et al.* (2012) Radiotherapy promotes tumor-specific effector CD8+ T cells via dendritic cell activation. *J Immunol*, **189**(2): 558-66.